DOI: 10.4149/km_2015_2_113

Analysis of microstructure and properties of Mg/Al dissimilar joints by GTAW with Al-Si filler wire

Du Hongyan, Li Yajiang*, Liu Guoliang, Xu Youxiao, Wang Juan

Key Lab of Liquid and Heredity of Materials, Ministry of Education, Shandong University, Jinan 250061, P. R. China

Received 27 February 2014, received in revised form 20 June 2014, accepted 26 June 2014

Abstract

Mg/Al dissimilar materials were welded successfully by gas tungsten arc welding (GTAW) using SAlSi-1 and SAlSi-2 welding wire. The joints with good surface forming and free of defects were achieved. The Mg/Al welded joints were analyzed by means of optical microscope, scanning electron microscope and micro-sclerometer. The results show that the fusion area on magnesium side is obviously divided into columnar crystal zone and dendritic crystal zone. More intergranular precipitates were observed in dendritic crystal zone than in columnar crystal zone. However, the weld area is the typical columnar zone. No high microhardness brittle phase was observed in the fusion area near magnesium side. The microhardness of weld zone is slightly higher than magnesium base metal, and far lower than the Al base metal.

Key words: dissimilar material, GTAW, microstructure, microhardness

1. Introduction

Magnesium and magnesium alloys are the relatively light-weight structure materials in industrial application and are one of the most potential materials in development and application of green engineering. When magnesium alloy is joined with other metal, it has some favorable characteristics such as low density, high specific strength, high modulus of elasticity, certain corrosion resistance and dimensional stability [1]. Aluminum alloys can be processed into various profiles owing to their low density and good plasticity. They are widely used in industry due to excellent electrical conductivity, thermal conductivity and corrosion resistance [2]. Moreover, with the wide applications of magnesium and magnesium alloys in the fields of aviation, automobile and instrument industries, the difficulties of welding magnesium alloy and aluminum alloy appear inevitably. The reliable welding joint with excellent properties of magnesium and aluminum alloys combines full priorities of the two dissimilar metals. It has an important theoretical significance and practical application value, and promotes the application of magnesium and magnesium alloy greatly.

At present, the welding methods of Mg/Al dissimilar metals include friction stir welding, diffusion welding, soldering, laser welding, etc. [3–6]. However, the pressure welding and brazing have special requirements on the size and shape of the workpiece, and their adaptability is not sufficient [7–8]. The fusion welding method is more flexible, and has high efficiency. However, GTAW welding method adopted leads to the formation of intermetallics that affects the weldability of joints [9–10]. In the paper, microstructure and properties of the Mg/Al dissimilar joints with Al-Si filler wire were observed and analyzed. It is aimed to realize the welding of Mg/Al dissimilar metals by gas tungsten arc welding (GTAW). The results can provide a research basis for the following researches on welding of dissimilar metals.

2. Experimental

7005 aluminum alloy and AZ31 magnesium alloy pipes were used as base materials. Both aluminum and magnesium alloys are 2.5 mm in thickness, and the external diameters are ø = 35 mm. The chemical compositions of base metals are listed in Table 1. SAlSi-1

*Corresponding author: tel./fax: +86 531 88392924; e-mail address: yajli@sdu.edu.cn

Table 1. Chemical composition of AZ31 and Al7005 alloys (wt.%)

Material	Chemical composition							
	Mg	Al	Mn	Zn	Be	Cu	Fe	Si
AZ31	other	3.19	0.334	0.81	0.01	0.005	0.005	0.02
7005	1.0–1.8	other	0.20–0.70	4.0–5.0	–	0.10	0.40	0.35

Table 2. Chemical composition of silicon aluminum wire (wt.%)

Type	Chemical composition									
	Si	Fe	Cu	Mn	Mg	Cr	Zn	Ti	Be	Al
SAlSi-1	4.5–6.0	0.8	0.30	0.05	0.05	–	0.10	0.20	0.05	other
SAlSi-2	11.0–13.0	0.8	0.30	0.15	0.10	–	0.20	–	0.05	other

Table 3. The processing parameters for GTAW welding

Welding wire	Welding current I (A)	Arc voltage U (V)	Flow of argon shield (L min^{-1})	Welding rate v (mm min^{-1})
SAlSi-1	40	15	5	5
SAlSi-2	46	15	5	2

and SAlSi-2 were used as welding wire. Influence of Si contents on microstructure and microhardness was investigated by the comparison of two kinds of welding wires. Main chemical compositions of welding wires are listed in Table 2. The welding of Mg/Al dissimilar metals was conducted using GTAW. The welding process parameters are listed in Table 3.

Before welding, the oxide films on the surface of 7005, AZ31 and welding wires were removed by grinding process. Oil contamination and other impurities were cleaned using the acetone. After welding, metallographic specimens were cut from the joint. The fusion zone in Mg side was etched using alcoholic solution with 5 vol.% nitric acid. The fusion zone on Al side was etched with chemical etchant ($HF : HNO_3 : H_2O = 2 : 3 : 5$, in volume ratio).

Microstructure of the weld zone was observed using optical microscope (OM) and scanning electron microscope (SEM). Element distribution in the joint was analyzed using electron probe microanalyzer (EPMA). The microhardness distribution in the Mg/Al joints was tested by micro-sclerometer.

3. Results and discussion

3.1. Microstructural characteristics of the fusion zone on Mg side

Figure 1 shows the microstructures and morphologies of the weld zone on Mg side obtained using SAlSi-1 welding wire. Figure 1a shows the microstructure morphology of the weld seam and HAZ on Mg side. The grain size of Mg substrate near the fusion zone is very small, and the Mg substrate around the tissue away from the fusion zone has not obviously changed. Fusion zone composed of half melting base metal and weld metal was formed between the weld seam and Mg substrate. A gray columnar zone with penniform structure was formed near the Mg substrate. The area near the weld seam center is composed of coarse dendrites, extending to the weld seam. And there is an obvious fusion line between the weld seam and base metal. The difference of the metallographic microstructure and detailed structure is shown in Fig. 1b. The fusion zone near Mg side could be divided into the columnar zone and the dendritic zone. And there are a lot of black lumps in the transition region between the columnar zone and the dendritic zone.

Figure 1c shows the SEM microstructure of the fusion zone near Mg side. The penniform zone is composed of fan-shaped meshed structures. More detailed structures are distributed between dendrites and crystalline structure. Mg substrate is mainly composed of αMg and γ-$Mg_{17}Al_{12}$ eutectic structure. The fusion zone with bright grains and that different from the base metal is nearly perpendicular to the base metal and grows from the fusion line to the weld seam.

Figure 2 is the microstructure of the fusion zone near Mg side by SAlSi-2 welding wire. Figure 2a de-

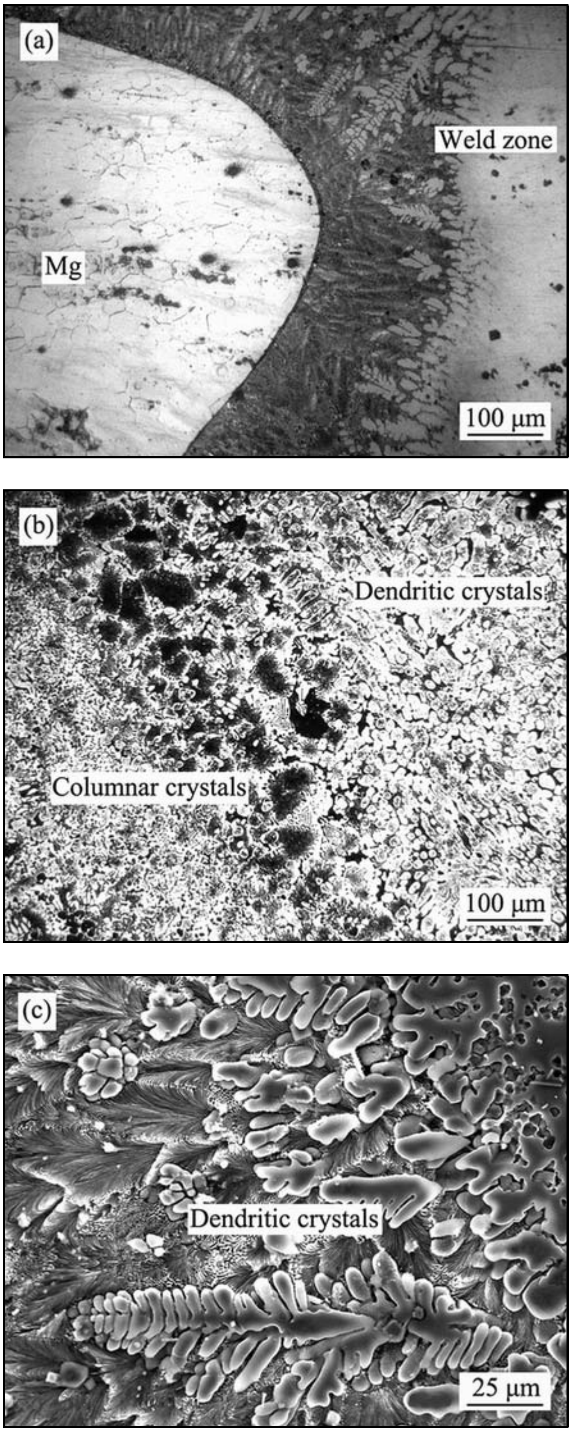

Fig. 1. Microstructure near the Mg side of Mg/Al joints by SAlSi-1 welding wire: microstructure of weld zone near Mg side (a), fusion zone near Mg side (b), SEM image of the fusion zone (c).

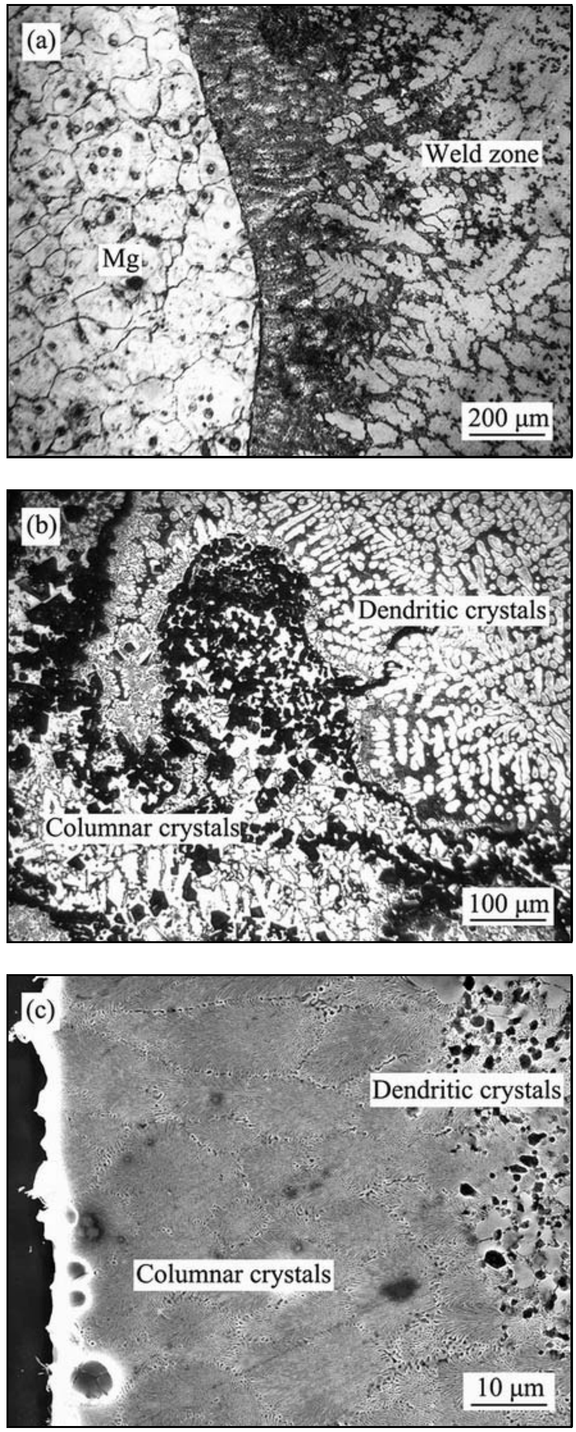

Fig. 2. Microstructure of Mg/Al joints near the Mg side by SAlSi-2 welding wire: microstructure of the joint on Mg side (a), fusion zone close to Mg side (b), SEM image of fusion zone (c).

picts the microstructure of the fusion zone on Mg side. Figures 1a and 2b show the microstructure morphology of the fusion zone on Mg side with an obvious fusion line. The fusion zone of the weld joint obtained by GTAW using SAlSi-1 welding wire can be divided into three different regions. However, the intergranular precipitates between dendritic crystals associate with increasing Si and Zn when using welding wire SAlSi-2. As a result, Mg and Si generate thick lump crystals of Mg_2Si phase, and Mg and Zn gener-

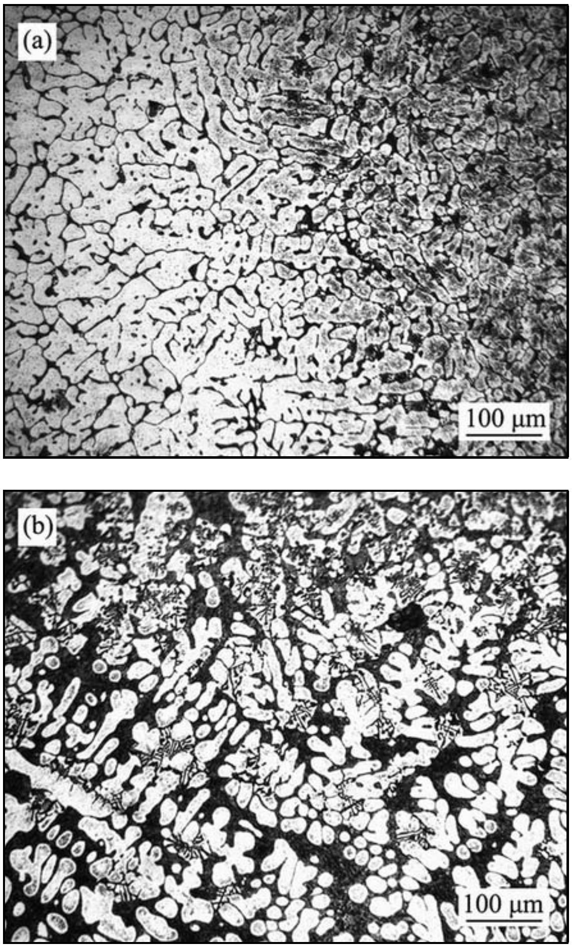

Fig. 3. Microstructure of the weld zone: microstructure of the weld seam by SAlSi-1 (a); microstructure of the weld seam by SAlSi-2 (b).

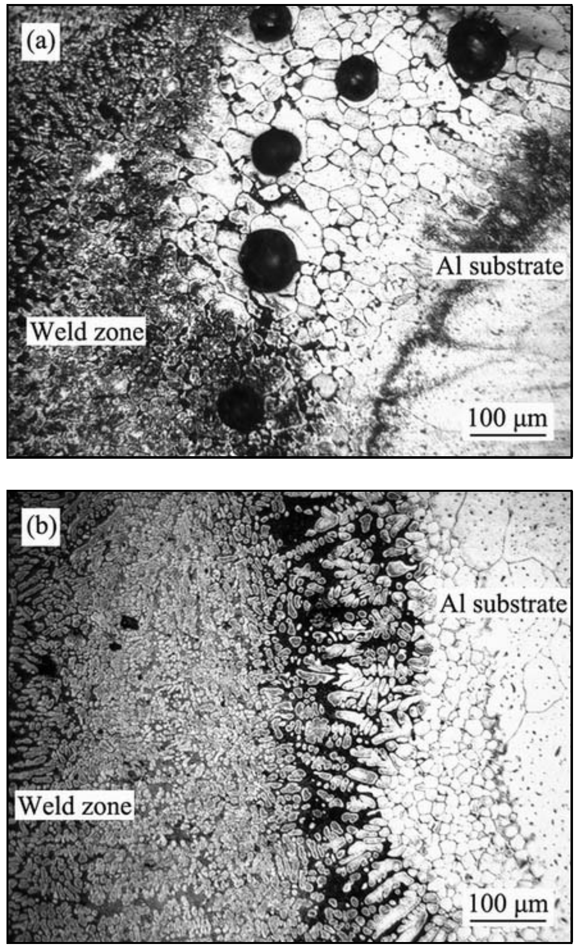

Fig. 4. Microstructure of the fusion zone on Al side: microstructure of fusion zone by SAlSi-2 (a), microstructure of fusion zone by SAlSi-1 (b).

ate stable compound $MgZn_2$ in crystalline region. Figure 2c shows the SEM image of the fusion zone on Mg side. The zone mainly contains intense columnar crystalline structure with little intergranular precipitates, and has some dendritic intergranular precipitates.

Figure 2 shows the microstructures and morphologies of the fusion zone on Mg side obtained by GTAW with SAlSi-2 welding wire. The microstructure and morphology shown in Fig. 2a are also different from those in Fig. 1a. Figure 2b shows the microstructure of fusion zone with clear crystal boundaries on Mg side. Since SAlSi-1 welding wire was adopted, less black lumps with dendritic shape are generated compared to Fig. 1. The solid solubility of Si in Mg is 0.03 % according to Mg-Si binary phase diagram. The content of Si in SAlSi-1 is 5 %, while in SAlSi-2 is around 12 %. The black lumps of dendritic intergranular precipitates are composed of Si and Mg_2Si. According to welding process, the dendritic crystalline region contains more intergranular precipitates and more complex structures compared to other regions, which results in the stirring and segregation of weld pool during welding.

3.2. Microstructural characteristics in weld seam and fusion zone on Al side

Figure 3a shows microstructure morphology of weld seam acquired by SAlSi-1 welding wire. There are coarse dendritic crystals on Mg side and fine dendritic crystals on Al side. According to macrostructure analysis, the formation of obvious boundary in weld seam center results from low welding current, fast speed and slow cooling rate. However, Fig. 4 shows the microstructure morphology of weld seam acquired by SAlSi-2 welding wire, which is a typical dendritic structure zone.

It can be seen from Fig. 4 that there is an obvious transition zone between aluminum substrate and weld seam. The transition zone of the joint by SAlSi-2 welding wire is much wider than that of the joint by SAlSi-1 welding wire. Based on the analysis of wire

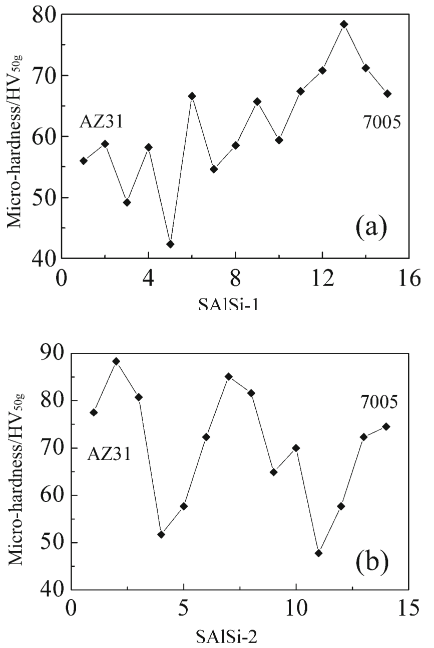

Fig. 5. Microhardness distribution of Mg/Al joint by GTAW: microhardness distribution by SAlSi-1 (a), microhardness distribution by SAlSi-2 (b).

component, the difference is associated with the contents of Si, Mn, and Zn. The grain size of weld seam is finer than that of aluminum substrate, which is mainly due to the small amount of alloying elements in the welding wire.

3.3. Microhardness distribution

The microhardness distribution of Mg/Al joints by GTAW with SAlSi-1 and SAlSi-2 welding wires was tested by microhardness tester, using a load of 50 g and a loading time of 10 s. The test results indicated that microhardness of Mg substrate was 62 HV_{50g}. The microhardness of weld seam near Mg side by SAlSi-1 is about 40–80 HV_{50g}, a little lower than the microhardness of 7005 aluminum substrate. The hardness of weld seam near Mg side by SAlSi-2 is about 40–90 HV_{50g}.

Moreover, it can be also seen that there is no big difference between the microhardness of the weld seam and base material. The microhardness of weld seam is a little higher than that of base material. The microhardness of weld seam basically fluctuates around 80 HV_{50g}. The black precipitate has lower microhardness, which fluctuates around 60 HV_{50g}. As for the weld seam, the Al-Si wire elements may have affected the structure, the refining grains have higher microhardness. Comparing the welded joint using Al-Si welding wire with butt welded joint without filler wire, the grain in the weld seam is much finer. Under the microhardness testing, the welded joint without filler wire has higher microhardness, with the maximum value about 250 HV_{50g}. However, the welded joint with Al-Si filler wire did not produce brittle phase, with the average microhardness value of 80 HV_{50g}. When the SAlSi-1 was used, γ-$Mg_{17}Al_{12}$ brittle phase did not exist in the fusion zone near AZ31 side, and Si, Mg and Al elements were formed into eutectic microstructure to reduce the amount of intermetallic compounds. Thus the microhardness in the fusion zone near AZ31 side was lower than that in AZ31 base metal. When the SAlSi-2 was used, eutectic silicon appears in the fusion zone near AZ31 side in addition to primary silicon, so the hardness in the fusion zone near AZ31 side was higher than that in AZ31 base metal. When the SAlSi-2 was used, the hardness close to AZ31 was higher than that using the SAlSi-1.

The shear strength test of the sample shows that low shear stress can cause fracture in the welding specimen by SAlSi-1, with the fracture position located on the side of the Mg substrate. The macro-morphology of fracture surface takes a bright white appearance with a large number of porosity. The fracture extends along the fusion line, and no plastic deformation is observed around the fracture. The fracture surface mainly contains coarse granular structure with metallic luster, which belongs to typical brittle fracture. When the same shear force on the welding specimen by SAlSi-2 was used, no brittle fracture was observed.

3.4. Component analysis of the fusion zone on Mg side by SAlSi-2

Figure 6 shows line scanning of the fusion zone on Mg side by SAlSi-2 with electron microprobe microscopy analyzer (EPMA). Two kinds of elements, mainly Mg and Al, exist in the fusion zone near Mg side. Content of Mg element is much higher than that of Al element in heat-affected zone near Mg side. Solid phase transformation occurred, and a few Al diffused into the heat-affected zone near Mg side. The content of Mg drops is quickly crossing the fusion line while the content of Al rises rapidly. The contents of Mg and Al are stable in the weld seam. Analysis shows that the main contents of molten Mg base metal are affected less by the weld seam in the fusion zone. Content mutations of Mg and Al occur in the fusion line, indicating no intermetallic compound is formed. Based on the little difference between microhardness of the regional zone and AZ31, it is shown that the regional zone, maybe $Mg_{17}Al_{12}$ + Mg structure, and Mg solid solution hybrid structures are formed according to Mg-Al binary alloy phase diagram analysis.

It also can be seen from the figure that the content of Si in the weld seam farther away from the base material is stable. This indicates that the addition of Si did not improve the microhardness of the fusion

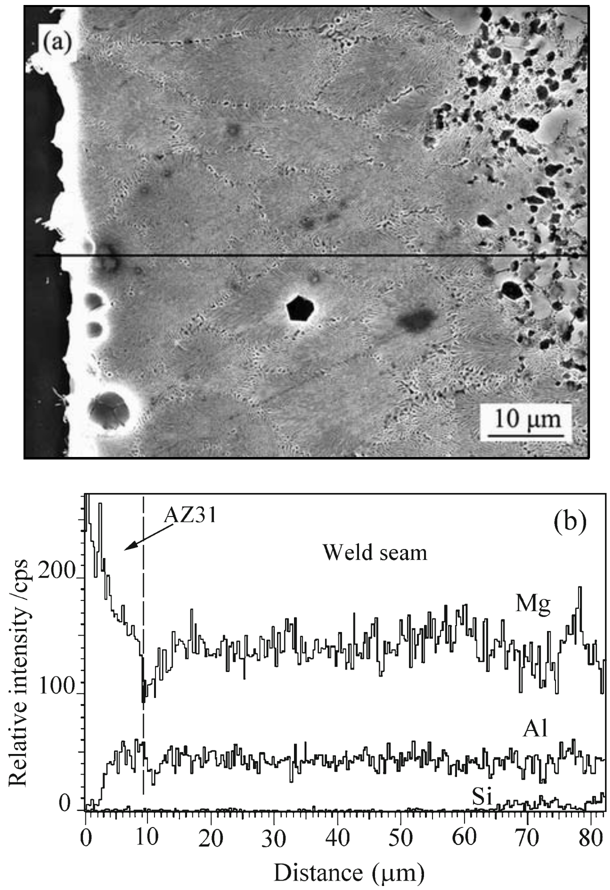

Fig. 6. Composition content of the fusion zone on Mg side by SAlSi-2.

zone during GTAW welding. Inter-diffusion of the elements between the welding wire and the base metal is reduced.

4. Conclusions

Mg/Al dissimilar joint can be successfully obtained by GTAW process using SAlSi-1 and SAlSi-2 welding wires. Due to the effect of base metal and filler wire, the microstructure of the weld seam is seriously uneven. The microstructure of weld seam close to the Mg side is obviously different than that near the Al side. The fusion zone at Mg side is the weak zone for mechanical performance of the joints. The microhardness of weld seam is approximately 80 HV_{50g}, which is slightly higher than that of base metal. The microhardness of gray precipitates is around 60 HV_{50g}. Moreover, when SAlSi-1 and SAlSi-2 welding wires are adopted, the microhardness distribution of the welded joint is uneven. But no obvious high hardness brittle phase was produced there. Through the analysis of the joints with SAlSi-1 and SAlSi-2 welding wires, more precipitates and higher microhardness values are observed in the joint using SAlSi-2 filled wire.

Acknowledgement

This research was supported by the National Natural Science Foundation of China (51175303). The authors express heartfelt thanks here.

References

[1] Wang, J., Li, Y., Liu, P., Geng, H.: Journal of Materials Processing Technology, *205*, 2008, p. 146. doi:10.1016/j.jmatprotec.2007.11.096

[2] Liu, P., Li, Y., Geng, H., Wang, J.: Materials Letters, *59*, 2005, p. 2001. doi:10.1016/j.matlet.2005.02.038

[3] Shapiro, A. E.: Welding Journal, *84*, 2005, p. 33.

[4] Chang, C. F., Das, S. K., Zedalis, M. S.: U.S. Patent, *5*, 1994, p. 332.

[5] Rattana, B.: Science and Technology of Advanced Materials, *6*, 2005, p. 199. doi:10.1016/j.stam.2004.11.014

[6] Wang, H., Liu, L., Liu, X.: Journal of Welding, *26*, 2005, p. 5.

[7] Yutaka, S. S., Seung, H. C. P., Masato, M.: Scripta Materialia, *50*, 2004, p. 1233. doi:10.1016/j.scriptamat.2004.02.002

[8] Liu, L., Tan, J., Liu, X.: Materials Letters, *61*, 2007, p. 2373. doi:10.1016/j.matlet.2006.09.016

[9] Schubert, E., Klassen, M., Zerner, T., Walz, C., Sepold, G.: Journal of Materials Processing Technology, *115*, 2001, p. 2. doi:10.1016/S0924-0136(01)00756-7

[10] Lu, L., Zhang, Y. F.: Journal of Alloys and Compounds, *290*, 1999, p. 279. doi:10.1016/S0925-8388(99)00221-2